Radiation-Induced Degradation of Si-CMOS Detector Aboard HIBARI Satellite in Low Earth Orbit

Minori Fukuda, Yoichi Yatsu, Kei Watanabe, Hiroyuki Kobayashi, Kiyona Miyamoto,
Yuki Amaki, Kenichiro Takahashi, Daiki Kobayashi, Yusaku Ozeki, Katsuki Tashiro, Ryo Saito, Yusei Kawaguchi,
Toshihiro Chujo, Hiroki Nakanishi, and on behalf of HIBARI Consortium
Tokyo Institute of Technology
2-12-1, Ookayama, Meguro, Tokyo, 152-8552, Japan; +81-03-5734-2388
petrel_uv@hp.phys.titech.ac.jp

Norihide Takeyama, Akito Enokuchi, Mai Shirahata, Toshiki Ozawa, Leo Terada
Genesia Corporation
3-38-3, Shimo-renjaku, Mitaka, Tokyo, 181-0013, Japan
takeyn@genesia.co.jp

Satoshi Hatori, Kyo Kume
The Wakasa Wan Energy Research Center
64-52-1 Nagatani, Tsuruga City, Fukui, Japan, +81-077- 24-5625
hatori@werc.or.jp

Kazuo Inaba
Inaba Digital Design
24-7-903 Yamashita-cho, Naka Ward, Yokohama, Kanagawa, Japan, +81-045-663-6478
inaba.kazuo@nifty.com

Toshinori Kuwahara, Shinya Fujita
Tohoku University
6-6-11, Aoba, Aramaki, Aoba, Sendai, 980-8579, Japan,
toshinori.kuwahara.b3@tohoku.ac.jp

Yuji Sato
ElevationSpace Inc.
F7, BIRTH KANDA, Takagi-Building, 1-17-1, Nishiki-cho, Chiyoda-ku, Kanda, Tokyo, Japan, +81-050-3669-1732
info@elevation-space.com

Junichi Kurihara
Hokkaido Information University
59-2, Nishi-Nopporo, Ebetsu, Hokkaido, Japan, +81-11-385-4411
kurihara@do-johodai.ac.jp

Yuji Sakamoto
Hokkaido University
Kita 8, Nishi 5, Kita-ku,Sapporo, Hokkaido,060-0808 Japan, +81-11-716-2111
yuji.sakamoto@eng.hokudai.ac.jp

Fumihiko Kamimura, Akira Masaki
Soliton Technology Corporation
2A Center East Building, 3-1-31 Chigasaki Minami, Tsuzuki-ku, Yokohama, Kanagawa, Japan, +81-045-945-7967
f.kamimura@soliton-technology.jp

Masakazu Yoshida, Shungo Hasumi, Tatsuya Fukuda
Tokai Engineering Service Co.,Ltd.
2-27-4 Kurokawa Hondori, Kita-ku, Nagoya, Aichi, Japan, +81-052-526-8092
yoshida@ja2.so-net.ne.jp

ABSTRACT

Degradation of Si-CMOS detectors of STTs in low earth orbit is presented. The 50kg microsatellite HIBARI was launched on November 2021, and designed for demonstrating a new attitude control method, named "Variable Shape Attitude Control (VSAC)". The attitude determination is therefore the key issue to evaluate the performance of VSAC. For this requirement, HIBARI possesses two star-trackers (STTs) equipped with Si-CMOS detectors. The space radiation environment in low Earth orbit poses significant challenges to Si-devices, which are susceptible to critical damage from exposure to high-energy protons. We have monitored the degradation of Si-CMOS of STTs aboard HIBARI for 2.5 years since its launch. Due to the limited bandwidth of RF-communication, we have only recorded the number of hot-pixels on the Si-CMOS detector, but with detector temperatures and the aim-point directions of STTs. First, we found that the number of hot-pixels strongly depends on the detector temperature, however it is inconvenient to evaluate the degradation because the temperature of STTs are not actively managed and varies by about ±7K every orbit. To evaluate the degradation tendency, we took into account the physical mechanism of activation of hot-pixels by radiations. For hot-pixel activation, defection formation due to non-ionizing interactions can be dominant effect. We proposed an empirical model describing the temperature-dependence of hot-pixel numbers based on the simple physical models. By making use of this model function, we calculated the number of hot-pixels at isothermal conditions of T=25°C. This clearly shows that the two STTs change its characteristics with exactly the same behavior in spite of different pointing directions, temperatures and parameter settings. Furthermore, we discuss the correlation between these damages and solar activity, as well as the correlation with imaging parameters. These results provide useful insight into the various Si-devices on board spacecraft.

INTRODUCTION

The space radiation environment is harsh for satellites and their onboard components. They can suffer significant degradation that can lead to critical failures. This is particularly a challenge for sensitive image detectors used in start trackers for attitude control and silicon devices used in scientific observations, as degradation accumulates as noise. In the Hubble Space Telescope (HST), it has been observed that high dark current pixels (so-called hot pixels) accumulate over time in orbit, posing serious challenges for some missions. [1-3]

For low Earth orbit missions, it must be considered that damage caused by high-energy protons from the inner Van Allen belt. Cosmic radiation originating from the sun and high-energy sources is trapped by the Earth's magnetic field, forming regions of high radiation density (Van Allen belts, radiation belts). Electrons with energies above 1 MeV are distributed in the outer belt at altitudes of 10,000 km to 20,000 km with a peak energy of 7 MeV. While trapped electrons also exist at altitudes below 10,000 km, their fluence is about one-tenth of the outer belt, and the peak energy is around 5 MeV. On the other hand, high-energy protons exceeding 100 MeV are distributed in the range of about 2,000 to 5,000 km in altitude (inner belt), have a serious impact on low-orbit satellites [4].

The radiation damage effects on Si devices are classified into three categories, i.e., total ionization dose effects (TID), single event effects (SEE), and displacement damage dose effects (DDD). TID is the accumulation of ionization effects in the gate insulator film of MOSFETs leads to characteristic changes such as an increase in Random Telegraph Noise (RTN) due to an increase in Si-SiO2 interface-traps, a shift in threshold voltage, and a decrease in mutual conductance [5]. Additionally, when high LTE (Linear Energy Transfer) particles such as α-rays and heavy ions enter semiconductor devices, high-density ionization charges are generated along the range. When part of these charges is collected by the electrodes, transient currents occur in the circuit and appear as SEEs that can cause transient malfunctions or permanent breakdown.[6]

Regarding the activation of hot pixels, DDD becomes dominant. High-energy protons recoils Si-atom nuclei in the detector bulk, and the resulting vacancies and interstitial atoms (Frenkel pairs) form point defects. Furthermore, if the energy of the recoiled atoms is high enough, a cascade of lattice defects form at the endpoints of the recoil path of the incident particles, leading to high-density defect clusters. These defects create trap levels within the bandgap of the depletion region, contributing to the increase in dark current.[7]
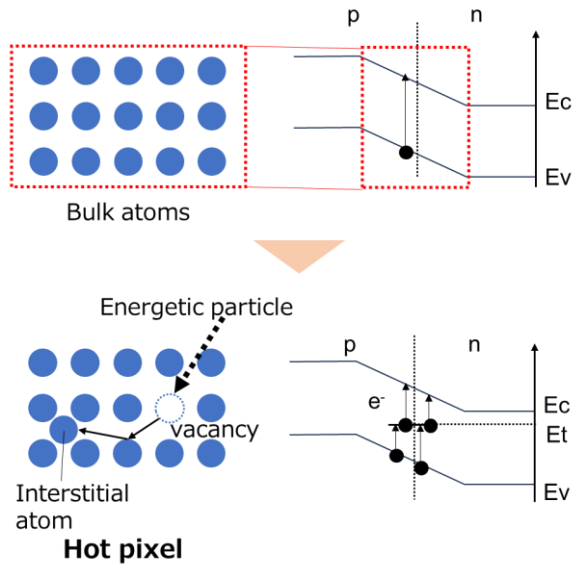
Figure 1: Displacement damage dose effect.

Figure 2: External View of HIBARI

Figure 3: Two STTs on board the Hibari satellite

MICRO SATELLITE "HIBARI"

The 50kg-class microsatellite "Hibari," mainly developed by Tokyo Institute of Technology, was launched on an Epsilon rocket in November 2021 as part of JAXA's Innovative Satellite Technology Demonstration-2 mission [8]. (Figure 1) The mission of the Hibari satellite is to demonstrate a novel attitude control method called "Variable Shape Attitude Control (VSAC)." To evaluate the performance of VSAC, attitude determination is a critical issue, so Hibari is equipped with two star trackers (STTs) (Figure 2).

These two STTs are of the same design, with 5M pixels, 2/3 size Si-CMOS detectors. However, they point in different directions: the anti-sun direction (STT_MZ) and the orbit orthogonal direction (STT_PXMY). We have been monitoring the degradation of the Si-CMOS in these two STTs over the two and a half years since launch. Due to the limited bandwidth of RF communication, a hot pixel detection algorithm was implemented on the onboard STTs, and the number of hot pixels was downlinked as telemetry data. Additionally, the temperature of the detectors and the pointing direction of the STTs during image acquisition were recorded.
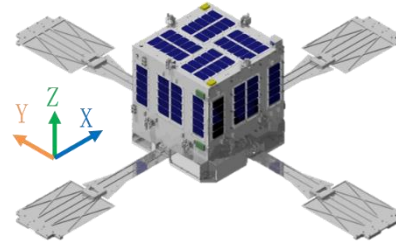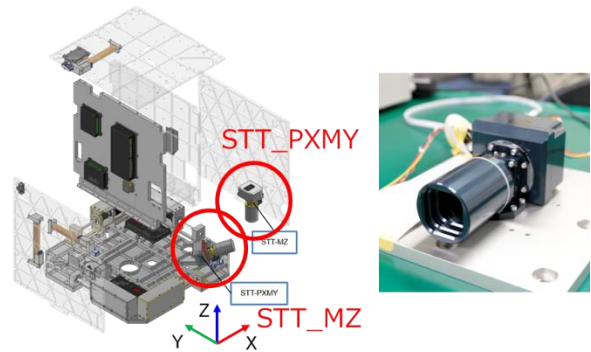
RESULTS AND DISCUSSION

Hot pixel count trends

Figure 3 shows the trend of hot pixel counts for the two CMOS sensors over two years since launch. For each separated area, the imaging parameters were changed while keeping the product of gain and exposure time constant. The two STTs showed exactly the same trend regardless of their pointing directions, and the number of hot pixels remained almost unchanged from 23/04 to 23/10, 13 months after the launch. The number of hot pixels at this time represented 0.2% of the total number of pixels in the sensor.

The variation in the number of hot pixels at each time point and the sharp increase in hot pixel count after 23/10 are thought to be due to the temperature dependence of the hot pixel count (Figure 4). The temperature of the STTs was not actively controlled and fluctuated by about ±7K per orbit, causing variations in the number of hot pixels at each time point. In addition, the sharp increase in hot pixel count was due to the rapid temperature increase. Since the number of hot pixels is strongly dependent on temperature, isothermal comparison is necessary to quantitatively evaluate the radiation-induced degradation trend. Therefore, we focused on the mechanism of hot pixel generation and modeled it according to its physics for evaluation.
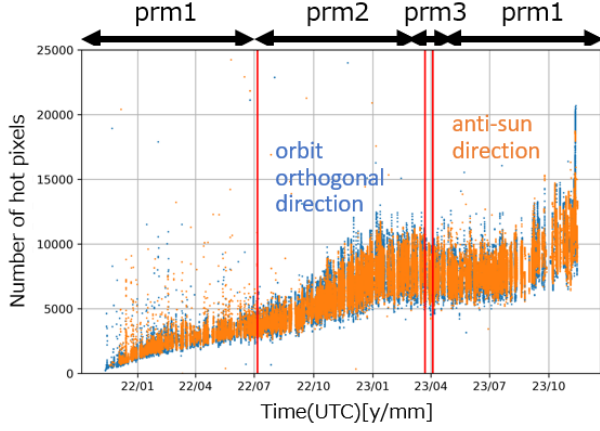
Figure 4: Hot pixel count trend of two CMOS sensors.

Table 1: Imaging Parameters

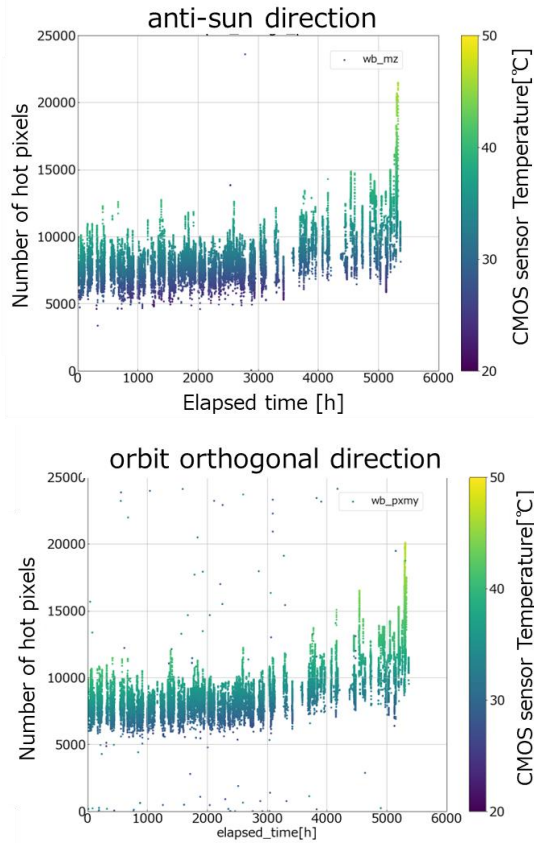| parameter	Prm1	Prm2	Prm3
Exposure time [ms]	50	75	90
Gain[dB]	10	6.48	4.86

Figure 5: The relationship between hot pixel count and sensor temperature

Analytical model

First, we examined the mechanism of hot pixel formation. Based on gamma-ray irradiation experiments, proton beam irradiation experiments on CMOS detectors conducted during the development process, as well as flight data, we inferred that hot pixels are mainly caused by interactions with high-energy charged particles in orbit. Lattice defects form new trap levels within the semiconductor bandgap (Figure), through which thermally excited electrons can easily transition to the conduction band.

This transition occurs through a competition of the following reactions (Shockley-Read-Hall kinetic):

a. Emission of electrons from the trap level to the conduction band

b. Trapping of electrons from the conduction band to the trap level

c. Trapping of holes from the valence band to the trap level. (emission of electrons to the valence band)

d. Emission of holes from the trap level to the valence band. (capture of electrons from the valence band)

where the reaction rates of each of the above $r_a, r_b, \cdots$, then the density change of free electrons in the trapped level is $\frac{dn_t}{dt} = -r_a + r_b - r_c + r_d$.
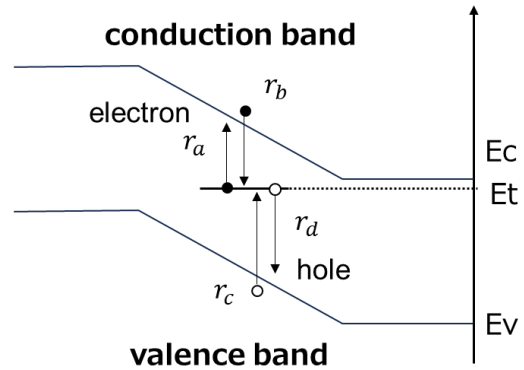

Figure 6: dark current model

Since the free carrier density in the depletion layer should be negligibly small due to the electric field, no free carrier supplementation to the trap level can be considered to occur, $\left(\frac{dn_t}{dt} = -r_a + r_d\right)$, and the electrons (holes) occupation probability of the trap level

can be expressed as the ratio of the emission rate of each carrier. As the rate of each transition is proportional to the carrier density, using the carrier density of electrons and holes in the trapped level (n_t, p_t), the emission rate of electrons and holes $\left(e_n, e_p\right)$ and the capture rate of electrons and holes (c_p, c_p), the following is expressed:

$$\frac{dn_t}{dt} = -e_n n_t + c_p p_t. \tag{1}$$

$$\left(p_t = \frac{e_n}{e_n + e_p} N_t, N_t: \text{Density of trapped levels}\right).$$

Furthermore, the conduction band, valence band, and carrier level are each considered to be in local equilibrium $\left(\frac{dn_t}{dt} = 0\right)$. For the rate of dark current generation, i.e., $r_a = e_n n_t = c_p p_t$, the deep trapping levels near the Fermi level become dominant and can eventually be expressed by the band gap energy E_g, as follows:

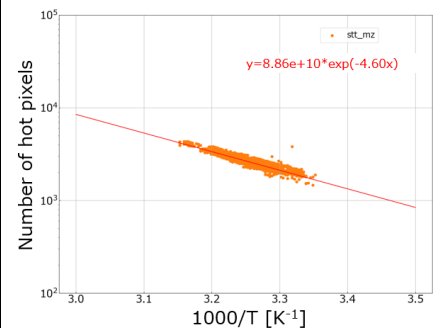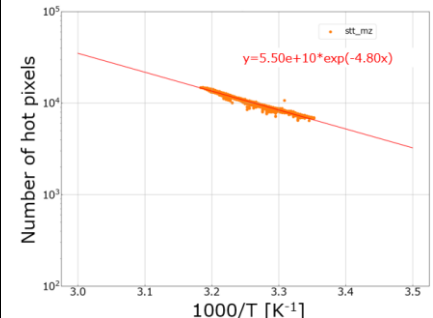$$D_e \propto D_0 \exp\left(-\frac{E_g}{2k_B T}\right). \tag{2}$$

This is derived using the fact that the electron energy distribution follows a Maxwell-Boltzmann distribution. Since the bandgap is equal in the same semiconductor, the number of electrons generated by individual lattice defects, i.e., the brightness value of the bandgap, can be expressed as an exponential function of temperature 1/T.

At high DDD, we should take into account the probability of having more than one defect per pixel, which leaves this model with D_0 degrees of freedom. However, from the measurement of sensor degradation due to radiation in orbit, it has been experimentally confirmed that this seems to follow a Poisson distribution. This is due to the small number of defects per pixel caused by displacement damage. [9]

Isothermal hot pixel count trend

The number of hot pixels acquired on an orbit is the number of bright spots above a certain threshold that are isolated on the screen. Therefore, this temperature dependence is proportional to Equation (2), regardless of the original brightness distribution of the hot pixel. Assuming the degree of radiation damage measured during the same period is the same, we derived the model function for the number of hot pixels each month (Table 1) and estimated the number of hot pixels at T=25 °C for each measurement period (Figure 7, The imaging parameters are changed for each area delimited by the red line. Error bars at 1 σ).

Table 2:   Model fit results of hot pixels

It can be seen that the number of hot pixels has continued to increase since launch, but the rate of change has become smaller. After about two years since launch, the number of hot pixels is about 6500 and 5500 for the anti- sun and orbital perpendicular STTs, respectively, which corresponds to 0.1% of the total sensor counts. Both STTs were damaged in almost the same manner, regardless of their pointing direction. Thus, this analysis allows a quantitative evaluation of the damage, excluding temperature effects.
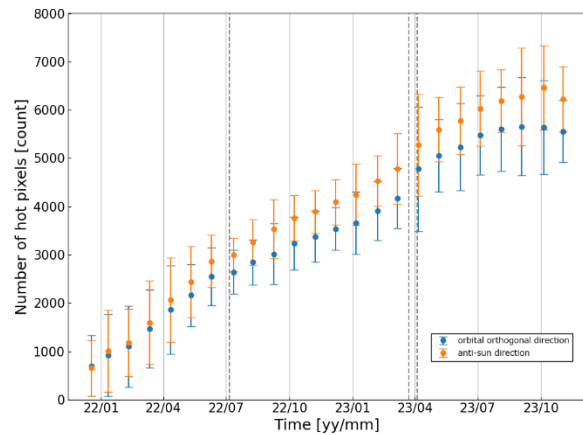

Figure 7: Hot pixel count trend equivalent to 25° C.

Comparison with solar activity

Finally, we compared the 25°C equivalent hot pixel increase rate with solar activity (Figure 8, The imaging parameters are changed for each area delimited by the red line. Error bars at 1σ). Solar activity data were sourced from the National Oceanic and Atmospheric Administration (NOAA). The number of sunspots and the 10.7 cm infrared flux are good indicators of solar activity, both of which are increasing during this evaluation period, when solar activity was approaching its maximum. In particular, there was no significant change in the rate of increase of hot pixels in the months of January and July 2023, when solar activity was especially high. In LEO at an altitude of 550 km, no clear correlation with solar activity can be confirmed.

With the exception of the period from April to June 2023, the rate of increase in hot pixels shows a decreasing trend. During the first six months after launch, the rate was increasing at about 400 per month (0.008% of the total sensors), but the rate gradually decreased to about 200 per month in the two years after launch. The rapid degradation at the beginning of the flight is presumably due to the defect generation rate and de-excitation (annealing) time constant caused by radiation. No failures were detected in the logic section of the STT during this period.
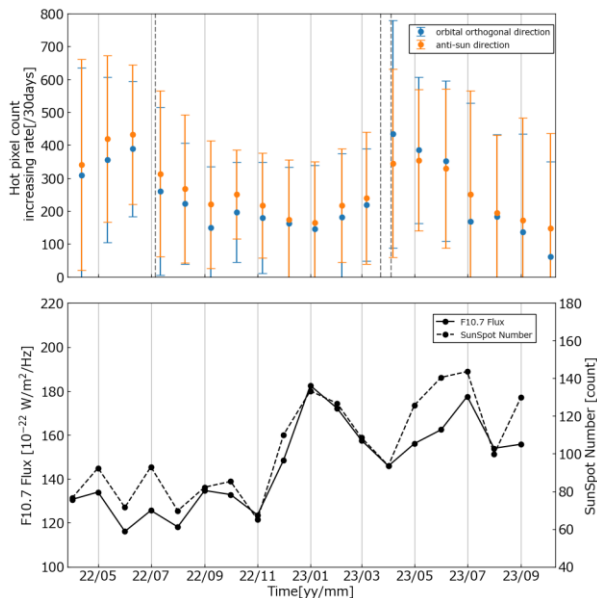

Figure 8: Hot pixel counts increasing per 30 days vs. solar activity (sunspot counts, F10.7 flux)

CONCLUSION

We recorded the displacement damage generated by the CMOS sensor onboard the Hibari satellite for as long as two years in orbit. In addition, a physical model enabled quantitative evaluation of the damage in microsatellites, which are generally subject to temperature fluctuations. These results provide useful insight into the various Si-devices on board spacecraft. Furthermore, it was confirmed that this STT has sufficient radiation tolerance in LEO, even though it is made of consumer products.

References

1. M. Sirianni, et al., "Characterization and on-orbit performance of the Advanced Camera for Surveys CCDs," Proc. SPIE 4854, pp. 496-506, 2003.

2. R. A. Kimble, P. Goudfrootij, and R. L. Gilliland, "Radiation damage effects on the CCD detector of the Space Telescope Imaging Spectrometer," Proc. SPIE 4013, pp. 532-544, 2000.

3. M. Clampin, G. Hartig, H.C. Ford, M. Sirianni, G. Meurer, A. Martel, J.P. Blakeslee, G.D. Illingworth, J. Krist, R. Gilliland, and R. Bohlin, "Status for the Advanced Camera for Surveys," 2002 HST Calibration Workshop, Space Telescope Science Institute, October 2002.

4. J.R. Schwank, "Basic Mechanisms of Radiation Effects in the Natural Space Environment", 1994 IEEE NSREC Short Course, 1994

5. T. R. Oldham and F. B. McLean, "Total Ionizing Dose Effects in MOS Oxides and Devices," IEEE TRANSACTIONS ON NUCLEAR SCIENCE, VOL. 50, NO. 3, 2003

6. J. R. Srour and J. M. McGarrity, "Radiation effects on microelectronics in space," Proc. IEEE, vol. 76, no. 11, pp. 1443–1469, Nov. 1988.

7. M. Moll, "Displacement damage in silicon detectors for high energy physics," IEEE Trans. Nucl. Sci., vol. 65, no. 8, pp. 1561–1582, Aug. 2018.

8. K. Watanabe, et al. "Initial In-Orbit Operation Result of Microsatellite HIBARI: Attitude Control by Driving Solar Array Paddles," 36th Annual Small Satellite Conference, 2002

9. C. Virmontois, et al." Similarities Between Proton and Neutron Induced Dark Current Distribution in CMOS Image Sensors," IEEE TRANSACTIONS ON NUCLEAR SCIENCE, VOL. 59, NO. 4, AUGUST 2012